



Design of High-Power Density Spoke-Type Interior Permanent Magnet Synchronous Motor for E-Bikes

Elektrik Destekli Bisikletler için Yüksek Güç Yoğunluğuna Sahip Çubuk Tipi Gömülü Mıknatıslı Senkron Motor Tasarımı

¹Yusuf YASA 

¹Istanbul Teknik Üniversitesi, Elektrik-Elektronik Fakültesi, İstanbul, Türkiye

¹yusufyasa@itu.edu.tr

Araştırma Makalesi/Research Article

ARTICLE INFO

Article history

Received : 22 May 2023

Accepted : 10 July 2023

Keywords:

Electrified bike, E-bike, high-performance electric motor, Spoke type interior permanent magnet synchronous motor.

ABSTRACT

In this paper, the high-performance electric motor is designed for e-bikes. Desired features from the electric motor are discussed and the required parameters such as outer diameter, stack length, operating speed, and torque are determined. High-power and high-torque densities at low-rated speeds are the most important required features in e-bike applications. In addition, the high dynamic mechanical response is also important as the motor should be synchronized with the user's foot activity. A design study is executed for a mid-drive e-bike traction system. The electromagnetic design study is started by determining the motor type and slot/pole configuration. Based on the required features, the spoke type IPM is chosen to be developed. Hereafter design tips are mentioned and electromagnetic analyses are performed through finite element analyses. The results show that the developed spoke-type interior permanent magnet motor (IPM motor) in the limited volume can run the bike efficiently and silently which are the signs of successful design.

© 2023 Bandırma Onyedi Eylül University, Faculty of Engineering and Natural Science. Published by Dergi Park. All rights reserved.

MAKALE BİLGİSİ

Makale Tarihleri

Gönderim : 22 Mayıs 2023

Kabul : 10 Temmuz 2023

Anahtar Kelimeler:

Elektrikli bisiklet, E-bisiklet, Yüksek-performanslı elektrik motoru, Çubuk-tipi gömülü mıknatıslı senkron motor

ÖZET

Bu yazıda, e-bisikletler için yüksek performanslı elektrik motoru tasarlanmıştır. Elektrik motorundan istenen özellikler tartışılmış; dış çap, laminasyon uzunluğu, çalışma hızı ve tork gibi gerekli parametreler belirlenmiştir. Düşük nominal hızlarda yüksek güç ve yüksek tork yoğunlukları, e-bisiklet uygulamalarında gereken en önemli özelliklerdir. Ayrıca, motorun kullanıcının ayak aktivitesi ile senkronize olması gerektiğinden, yüksek dinamik mekanik cevap önemlidir. Ortadan çekişli bir e-bisiklet çekiş sistemi için bir tasarım çalışması yapılmıştır. Elektromanyetik tasarım çalışmasına motor tipi ve oluk/kutup konfigürasyonu belirlenerek başlanır. İstenen özellikle dikkate alınmış, geliştirilmek üzere çubuk tipi gömülü mıknatıslı senkron motor (IPM motor) seçilmiştir. Sonrasında, tasarım ipuçlarından bahsedilmiş ve elektromanyetik analizler sonlu eleman analizleri ile gerçekleştirilmiştir. Elektrik destekli bisiklette sınırlı bir hacimde çalışacak şekilde geliştirilmiş olan bu çubuk tipi gömülü mıknatıslı senkron motor, analiz sonuçlarından da anlaşıldığı üzere, elektrikli bisikletin ihtiyaç duyduğu tüm çalışma rejimlerinde yüksek verimli ve sessiz/konforlu şekilde çalışmaktadır.

© 2023 Bandırma Onyedi Eylül Üniversitesi, Mühendislik ve Doğa Bilimleri Fakültesi. Dergi Park tarafından yayınlanmaktadır. Tüm Hakları Saklıdır.

1. INTRODUCTION

The bicycle is one of human history's most aged and used vehicles. The time of its invention is not clear but probably around the 18th century according to the most common view. People usually start using bikes at very early ages and do not give up on their life span.

Electric vehicles are now very popular in the 21st century with electrified cars. The main reason is the oil depletion in the world. Moreover, electric vehicles are usually more comfortable and less costly than conventional internal combustion engines. The awareness of environmental pollution is another big reason for the people.

Electrified bikes are now a new trend nowadays. The technology is based on supporting cyclists when he/she has difficulty in driving the ride such as climbing hills. The application term is named “electrically assisted e-bike” in the literature. The assisted electric motor can be mounted in three places, as shown in Figure 1. The first one is called a mid-drive electric motor-assisted bike. However, the second and third names are hub-motor-assisted e-bikes. Hub motors can be located on either the rear wheel or the front. Each option has several advantages and disadvantages. Front-hub motors provide a pulling sensation to the rider which is most usual and the same as front-wheel cars. Despite this, the rear hub makes feeling like a “pushing” which is not subject to choice for some people. Front-hub motors require less maintenance and provide easy installation as there is no chain or gear in the front wheel. However, spinning out is also easier than the rear-hub option as the weight is concentrated on the front side.

The rear side of the frame in the bike is usually much stronger than the front side. Hence, there is the possibility to put a much more powerful electric motor in the front-side hub. Moreover, as the front wheel can rotate, mounting the torque sensor pedal assist is not possible in the front-hub option. Torque sensor offers exclusive skills to the bike. With a torque sensor, the controller can control the electric motor to assist the rider with support. So, the rider can feel the uphill road as a straight road where the electric motor provides differential force between the two road types. However, the installation of the rear-hub motor is not straightforward.

The third alternative driving method is the mid-drive system. Here, standard wheels and drive-train including chains and gears can be used. Just the electric motor is added to the mid-frame.

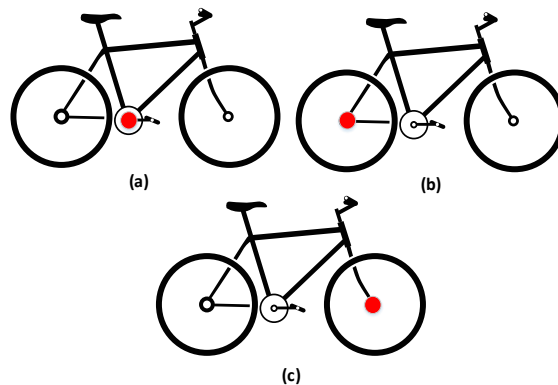


Figure 1. The mounting plates of the electric motor in the bike.

In the motion flow diagram, as the electric motor exists before the gear and chain, the electric motor speed is usually in the optimum range. This is adjusted either by the rider or the controller automatically. Moreover, the rider feels more like a natural bike in the mid-drive. As the electric motor is in the middle of the frame, the bike weight is more balanced than front or rear-hub e-bikes. As the electric motor-gear shaft is directly integrated with the pedals, the aggressive behavior by the riders may increase the wear in the system which may cause faster maintenance [1].

In the e-bike drive system, a permanent magnet synchronous motor (PMSM) is mostly preferred. In some academic research [2]–[5], switched reluctance electric motor is proposed as traction. Switched reluctance motors can provide high torque density and high efficiency with a cheap production cost. As an alternative to the PMSM, the absence of the magnet cost plays a key role in the cost advantage. However, the torque ripple may cause a bad feeling which results in comfortless driving for the rider. In PMSM-assisted e-bikes, internal or external rotor types can be used [6]. Outer rotor PMSMs are typically used in the front or rear hub-assisted e-bikes. However, in mid-drive applications, internal rotor PMSM is popular [7]–[10]. Advancements in e-bikes are going parallel with electric vehicle technology. In [3], [11]–[13], the researchers proposed regenerative braking which will make the e-bike more efficient and increase driving mileage. Charging the battery is another challenging subject for researchers. In [14]–[17] the charging methods including wireless power transfer are studied.

In this study, a spoke-type interior permanent magnet synchronous motor is developed for e-bikes. The desired features of the electric motor are mentioned then a step-by-step design study is discussed for e-bike applications. Finally, the results are discussed in the conclusion section.

2. DESIRED FEATURES FROM THE E-BIKE ELECTRIC MOTOR

Electrified bikes are getting famous nowadays at affordable prices. Comfort level is getting a rise in bikes with electrifying. There is no doubt the high-performance electric motor in the e-bike system plays an important role in that comfort level. The desired features from the mid-drive system are,

1. High power density (W/kg),
2. High torque output at low speed,
3. Low-rated speed (around 100rpm),
4. Low weight,
5. Waterproof,
6. Quick response,
7. Resistant to mechanical shock,
8. Durable,
9. Long maintenance period.

The weight of the bike is one of the important issues which determines the comfort level of the rider. Usually, conventional un-electrified bikes have a 12-14 kg weight. The electrification system includes a drive unit, onboard computer and controller, lithium-ion battery, and sensors. Table 1 shows two market players' drive unit specifications. Usually, the drive unit power is chosen as 250W. All brands have a reduction in the drive unit to increase the torque and reduce the operating speed. As the volume and diameter are limited with an application, the only way is designing the electric motor with high speed and relatively lower torque than increasing the torque level by using gear. Most of the batteries in the e-bikes have a 36V voltage level and 400Wh energy storage. Adding the drive unit and battery to the bike almost increases the system weight by around 50%.

Table 1. E-bike drives unit specifications in two famous brands.

	Yamaha	Bosch	
Battery			
Capacity	400	400	Wh
Weight	3	2.5	kg
Voltage	36	36	V
Battery range	95	90	km/average
Battery type	Lithium-ion		
Drive unit			
Output Power	250	250	W
Weight	3.1	2.9	kg
Torque	70	30	Nm
Torque (e-motor)	21.7	12	Nm
Gear ratio	3.22	2.5	
Speed (reduced)	110	100	rpm
Speed (e-motor)	354.2	250	rpm

In this study, a permanent magnet synchronous motor is selected to develop an e-bike drive unit. Permanent magnet synchronous motors (PMSMs) offer several advantages over other types of electric motors. Some key advantages of PMSMs are high efficiency, high power density, excellent speed and position control, wide speed range, high torque density, rapid dynamic response, and regenerative braking capability. Overall, the advantages of PMSMs make them well-suited for a wide range of applications that require high efficiency, precise control, compact size, and high torque output.

The drive unit design specifications are given in Table 2.

Table 2. E-bike drives unit specifications in two famous brands.

Drive Unit	Proposed study	
Capacity	400	Wh
Voltage	36	V
Output Power	250	W
Torque (gear output)	24	Nm
Torque (motor shaft output)	6	Nm
Gear ratio	4	
Speed (reduced)	100	Rpm
Speed (e-motor)	400	Rpm
Diameter	90	mm
Length	50	mm

3. PERMANENT MAGNET SYNCHRONOUS MOTOR DESIGN

Determining the number of slots and poles is the first step in the motor design. As the rated rotational speed is relatively lower than conventional electric machines, a high number of poles is usually preferred to keep the power density high. So the number of poles should be inversely proportional to the rated speed. In high rotational speeds, to limit the commutation frequency and iron losses, the number of poles should be kept low. However, in this application, the number of poles is maximized.

In PMSMs, there are several rotor types. Here, embedded magnet rotor configuration is selected to use the reluctance torque component effectively which provides high torque and power densities. Moreover, it is a relatively low-cost fabricated design. Spoke type rotor configuration is selected to continue design steps.

Cogging torque, also known as detent torque or reluctance torque, refers to the phenomenon in electric motors where there is a pulsating or non-uniform torque output during rotation. It occurs in motors with salient pole construction, such as permanent magnet motors or reluctance motors. The cogging torque arises due to the interaction between the magnetic field generated by the stator and the permanent magnets of the motor. When the rotor teeth align with the stator poles, there is an increase in magnetic reluctance, causing a variation in the magnetic flux density and resulting in a torque disturbance. This irregular torque can cause mechanical vibrations, and noise, and affect the smoothness of motor operation. Cogging torque is generally undesirable because it can degrade the motor's performance and efficiency, particularly at low speeds. It can also lead to position errors in motion control applications. Therefore, efforts are made in motor design and control techniques to minimize cogging torque. These methods include optimization of the motor geometry, selection of appropriate pole and slot configurations, and the use of control algorithms that compensate for or suppress cogging effects.

The cogging torque should be kept in a limited range to make the movement smooth and have low acoustic noise. There are several cogging torque minimization methods in literature such as skewing the stator lamination, skewing the magnets, chamfering the edges of the magnet surface geometry, etc. However, these methods make motor production more difficult. An easier cogging torque minimization method is concealed in configuring the appropriate slot/pole number. In this case, the fractional-slot configuration is always preferred to minimize the cogging torque. For the minimum cogging torque goal in three-phase PMSMs, appropriate slot/pole numbers are given in Table 3 [18]. An 18/16 slot/pole is selected for this application.

Table 3. Appropriate slot/pole number configuration for minimum cogging torque[18] for three-phase PMSMs.

0.75		1.125		1.5	
slots	poles	slots	poles	slots	poles
3	4	9	8	3	2
6	8	18	16	6	4
9	12	36	32	9	6
12	16			12	8
15	20			15	10
18	24			18	12
21	28			21	14
24	32			24	16
2.25		3		3.75	
slots	poles	slots	poles	slots	poles
9	4	6	2	15	4
18	8	12	4	30	8
27	12	18	6	45	12
		24	8		
		30	10		
		36	12		
4.5		5.25		6	
slots	poles	slots	poles	slots	poles
9	2	21	4	12	2
18	4	42	8	24	4
27	6			36	6
36	8			48	8

After determining the outer diameter, length, and number of slots and poles, the stator's inner diameter and air gap will be decided. As it is known from (1), generated torque in an electric motor is a function of the rotor outer diameter with a square relation. However, torque is proportional to the stack length. Hence, high torque-density electric machines are always designed with large diameters but short lengths. However, there is a space limit in rotor diameter. Based on experience, in spoke-type PMSMs, the rotor diameter can be kept larger than the usual surface PMSMs with high-energy magnets.

$$T = \sigma\pi DL \frac{D}{2} = \frac{\pi}{2} D^2 L \sigma \tag{1}$$

The geometry of the PMSM is optimized based on maximizing efficiency and minimizing the cogging torque and current density. The variation of the efficiency and current density in response to the magnet width is given in Figure 2 and Figure 3, respectively. Efficiency is increasing with magnet width however the rising edge is desaturating after some points. As the mechanical output power emerges with the production of the rotor and stator magnetic fields via $\vec{B}_r \times \vec{B}_s$, With rising magnet width, the required magnetic field from the stator, \vec{B}_s is decreased. So, the required current and the current density is reduced, as well.

Figure 4 and Figure 5 show the efficiency and cogging torque variation with a function of magnet thickness. With an incremental magnet thickness, the efficiency rises higher than the width. However, saturation starts around 1mm magnet thickness. Large magnet volume causes cogging torques as shown in Figure 5. However, as the cogging torque is minimized by selecting a fractional slot/pole ratio, the cogging level is in ignorable levels.

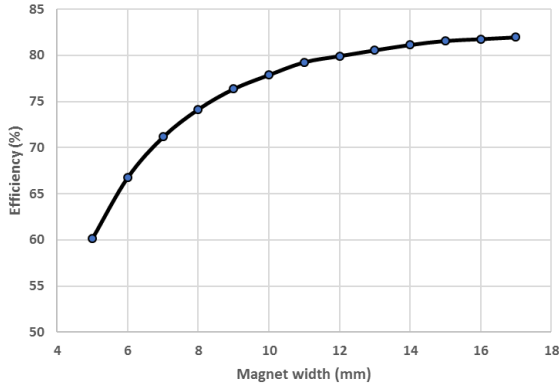


Figure 2. The variation of the efficiency with response to the magnet width.

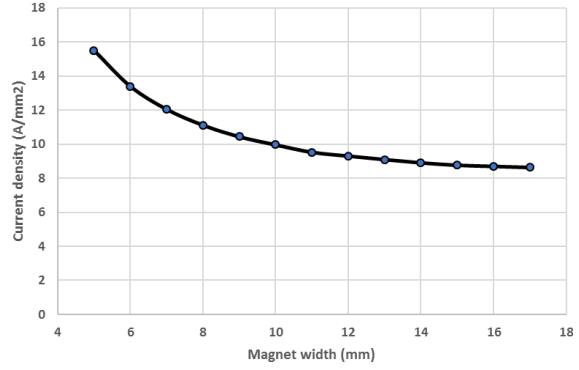


Figure 3. The variation of the current density in response to the magnet width.

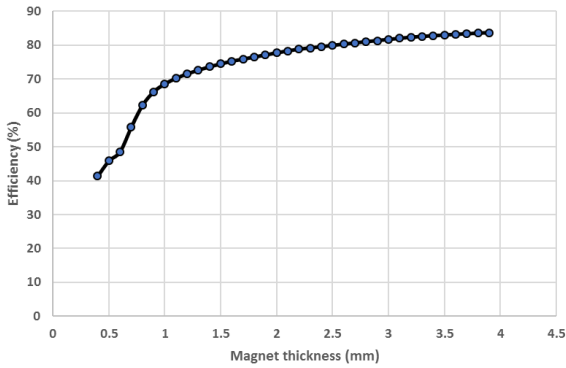


Figure 4. The variation of the efficiency with response to the magnet thickness.

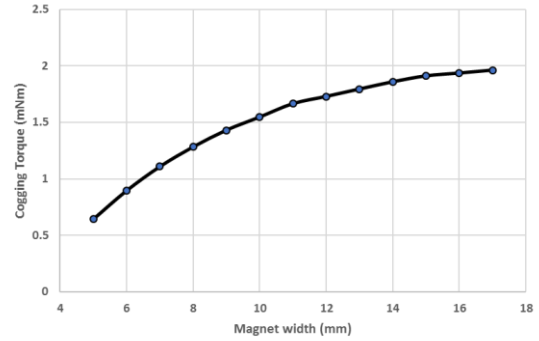


Figure 5. The variation of the cogging torque with response to the magnet thickness.

One of the most important parameters which play an important role on the efficiency is the number of conductors per slot. The conductor number determines the nominal or rated operating speed. Figure 6 and Figure 7 show the efficiency and rated torque parameters as a function of the number of conductors per slot. 28 conductors maximize efficiency. However, the corner speed where the rated torque starts to decrease is coming up with 40 conductors as shown in Figure 7.

Slot opening or clearance is useful for winding assembly to the stator. More clearance means easier winding assembly. However, the clearance deteriorates the magnetic field in the airgap and concentrates the magnetic field into the tooth which increases the cogging torque. Airgap magnetic field deterioration results in efficiency reduction as well, as shown in

Figure 8. Slot clearance with 2.2 mm is selected as an optimal point. The final geometry of the spoke-type PMSM is given in Figure 9. For 2D finite element analysis (FEA), meshing of the geometry is executed, initially. Mesh settings play a crucial role in getting accurate results. As the energy conversion place is the air gap between the stator and rotor, meshes in the air gap should be the smallest in the geometry. The magnets and the stator and rotor lamination are the second-order priorities after the air gap. Moreover, if the excited electrical frequency was high, the meshes on the lamination corners would be small to see the effect of the leakage. However, in this study, the excitation frequency at the rated speed is 53.33 Hz. Thus, the meshes on the corners are chosen as regular size same as lamination. Figure 10 shows the meshes on the quarter motor geometry.

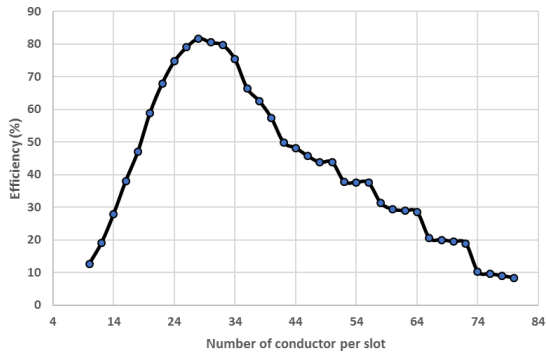


Figure 6. The variation of the efficiency in response to the number of conductors per slot.

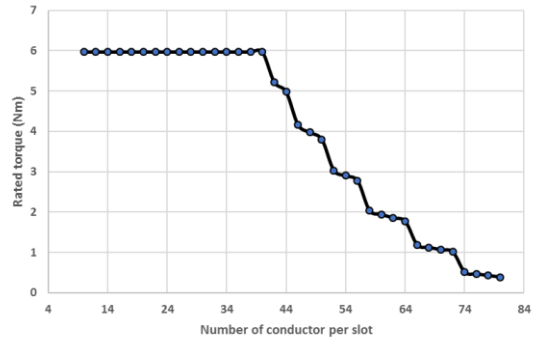


Figure 7. The variation of the rated torque in response to the number of conductors per slot.

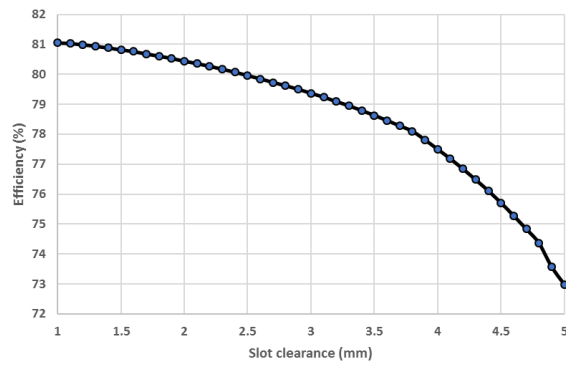


Figure 8. The variation of the efficiency in response to the slot clearance.

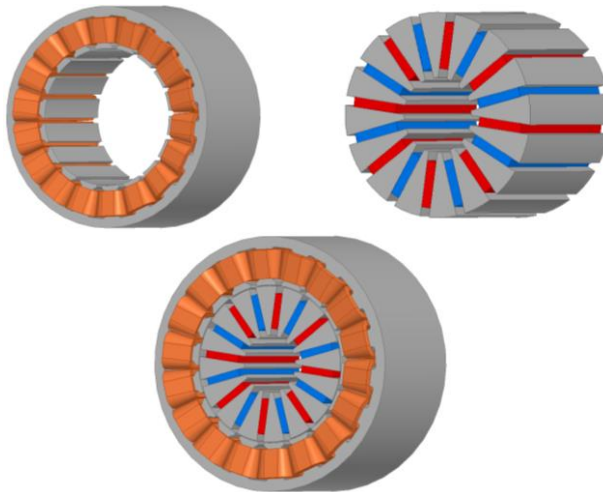


Figure 9. Designed spoke-type PMSM geometry.

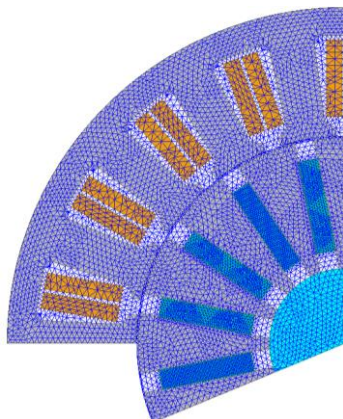


Figure 10. The meshing of designed spoke type PMSM for 2D FEA setup.

In 2D FEA analysis, cogging torque variation is plotted versus time. Figure 11 shows two electrical periods cogging torque data. From peak to peak there is a 0.2 Nm cogging value. Compared to the 6 Nm rated torque, 3.3% percent cogging is reported which will not be felt by the rider in terms of mechanical force and acoustic noise. For smooth motor control, the back EMF waveform is important. Figure 12 shows the back EMF waveforms of three phases at 400rpm operating speed. The fast Fourier Transform (FFT) analysis is performed for the one-phase back-EMF as given in Figure 13. The fundamental back-EMF magnitude is 13.11V and the total harmonic distortion of the back-EMF is 5.87%.

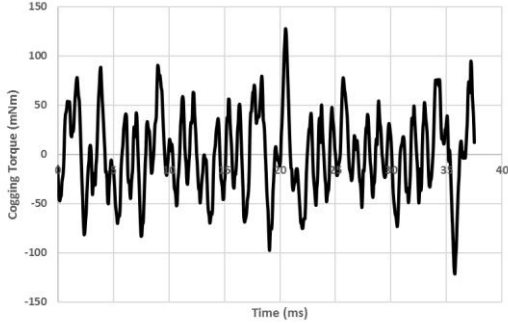


Figure 11. 2D finite element analysis result; cogging torque variation.

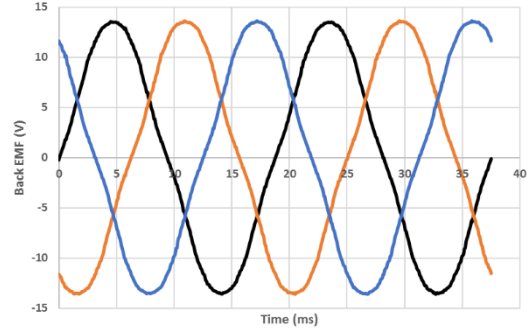


Figure 12. 2D finite element analysis result; Back-EMF variation.

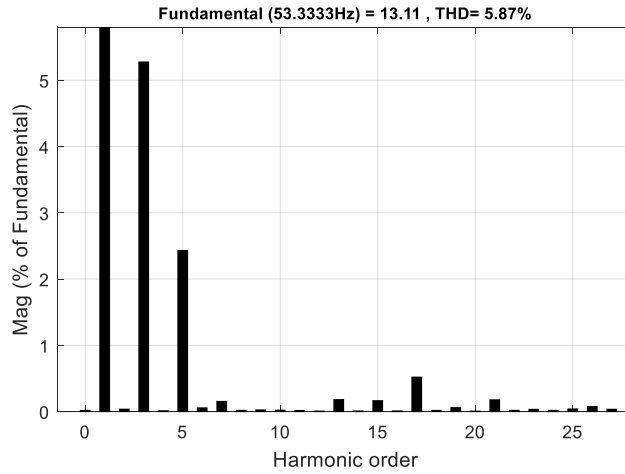


Figure 13. 2D finite element analysis result; Back-EMF fast Fourier transform total harmonic distortion result.

4. CONCLUSION

In this study, a spoke type of interior permanent magnet synchronous motor is developed using finite element analysis for electrified bike applications. High power/torque density at low speeds is one of the required challenging issues in e-bikes. Hence, with a minimum volume, the efficiency is maximized with parametrical analyses of the motor geometry. At e-bike applications, the required motor feature should not be focused only on the efficiency and power/torque density. High dynamic response with low mechanical inertia, low cogging torque, low torque ripple, low harmonic content in back EMF are important performance outputs, as well. The pedelec applications limits the motor output power at 250W and the maximum speed at 25 km/hour. The designed e-bike traction mechanical system is developed with 4 gear ratios. Hence, the rated motor speed is 400 rpm. At these particular conditions, the motor efficiency is reached to 81%. Moreover, critical design tips are mentioned considering e-bike requirements such as minimizing the cogging torque, maximizing the efficiency, etc. From the FEA results, 3% cogging torque is reached with fractional 18/16 spoke PMSM. The FFT analysis is executed on the back-EMF waveform. A 5.87% total harmonic distortion at the rated conditions is reported. The results show that developed spoke-type IPM in the limited volume can run the bike efficiently and silently which are the signs of successful design.

Author's Contribution

Yusuf YAŞA contributed to the design and implementation of the research, to the analysis of the results, and to the writing, reviewing, and editing of this manuscript.

Conflict of Interest

All authors declare that they have no conflicts of interest.

KAYNAKÇA

- [1] "https://momentummag.com/types-of-ebikes/," 2022-09-19, Date accessed.
- [2] B. Howey, E. Rowan, B. Bilgin, and A. Emadi "Thermal Trade-off Analysis of an Exterior Rotor E-Bike Switched Reluctance Motor," *Itec* 2017, pp. 605–612, 2017.
- [3] X.L.X. Liu, C.L.C. Liu, M.L.M. Lu, and D.L.D. Liu "Regenerative braking control strategies of switched reluctance machine for electric bicycle," *Int. Conf. Electr. Mach. Syst.*, pp. 3397–3400, 2008.
- [4] J. Lin, N. Schofield, and A. Emadi "External-Rotor Switched Reluctance Motor for an Electric Bicycle," *IEEE Trans. Transp. Electrification*, vol. 1, no. 4, pp. 348–356, 2015.
- [5] J. Lin, N. Schofield, and A. Emadi "External-rotor 6 #x2013;10 switched reluctance motor for an electric bicycle," *Ind. Electron. Soc. IECON 2013 - 39th Annu. Conf. IEEE*, pp. 2839–2844, 2013.
- [6] W. Chlebosz, G. Ombach, and J. Junak "Comparison of permanent magnet brushless motor with outer and inner rotor used in e-bike," *19th Int. Conf. Electr. Mach. ICEM 2010*, 2010.
- [7] A. Christen and V.V. Haerri "Analysis of a six- and three-phase interior permanent magnet synchronous machine with flux concentration for an electrical bike," *2014 Int. Symp. Power Electron. Electr. Drives, Autom. Motion, SPEEDAM 2014*, pp. 1251–1255, 2014.
- [8] V. Naveen Kumar, A. Syed, D. Kuruganti, A. Egoor, and S. Vemuri "Measurement of position (angle) information of BLDC motor for commutation used for e-bike," *Proc. 2013 Int. Conf. Adv. Electron. Syst. ICAES 2013*, pp. 316–318, 2013.
- [9] R. Meireles, J. Silva, A. Teixeira, and B. Ribeiro "An E . Bike Design for the Fourth Generation Bike - Sharing Services," *2013 World Electric Vehicle Symposium and Exhibition (EVS27)*, pp. 1–6, 2013.
- [10] R. Jiang, J. Zhang, G. Zhao, and C. Wu "Enhancing speed estimation accuracy of electric bike riders through training," *2014 17th IEEE Int. Conf. Intell. Transp. Syst. ITSC 2014*, pp. 1915–1916, 2014.
- [11] E. Ceuca, G. Brezeanu, and V. Trifa "Study for developing the energy recovering circuit for modern e-bike controller," *Proc. Int. Semicond. Conf. CAS*, vol. 2015–Decem, pp. 245–248, 2015.
- [12] E. Ceuca, I. Pocan, and O. Pop "Electromagnetic Compatibility Analysis of the Assembly e-bike - Power Electronic Converter with Recovery Function," no. December 1918, pp. 398–401, 2016.
- [13] N. Hatwar, A. Bisen, H. Dodke, A. Junghare, and M. Khanapurkar "Design approach for electric bikes using battery and supercapacitor for performance improvement," *IEEE Conf. Intell. Transp. Syst. Proceedings, ITSC*, no. Itsc, pp. 1959–1964, 2013.
- [14] L.A.L. Cardoso, M.C. Martinez, A.A.N. Meléndez, and J.L. Afonso "Dynamic inductive power transfer lane design for E-Bikes," *IEEE Conf. Intell. Transp. Syst. Proceedings, ITSC*, pp. 2307–2312, 2016.
- [15] H. On, T.H.E-bike, and U. Di "Ride by Wire Build a push- electronic bicycle shifter on the cheap," no. may, 2013.
- [16] K. Sangani "E-Bikes Take Off," *Eng. Technol.*, vol. 6, no. June, pp. 34–35, 2009.
- [17] L. Celentano, D. Iannuzzi, and L. Rubino "Controller design and experimental validation of a power charging station for e-bike clever mobility," *Conf. Proc. - 2017 17th IEEE Int. Conf. Environ. Electr. Eng. 2017 1st IEEE Ind. Commer. Power Syst. Eur. IEEEIC / I CPS Eur. 2017*, pp. 1–6, 2017.
- [18] T.J.E.M.J.R. Hendershot "Design of Brushless Permanent-Magnet Motors", Chelsea, Michigan: Oxford University Press, 1994.